

## Ultra-relativistic nuclear collisions

---

**A. Kalweit**<sup>a,\*</sup>

<sup>a</sup>*Experimental Physics department CERN,  
Esplanade des particules 1, Meyrin, Switzerland*

*E-mail:* [Alexander.Philipp.Kalweit@cern.ch](mailto:Alexander.Philipp.Kalweit@cern.ch)

Ultra-relativistic nuclear collisions provide unique opportunities to study quantum chromodynamics at extreme temperatures and densities. In this contribution, an overview of selected recent results and developments will be given along with a brief general introduction to the field.

*The European Physical Society Conference on High Energy Physics (EPS-HEP2023)  
21-25 August 2023  
Hamburg, Germany*

---

\*Speaker

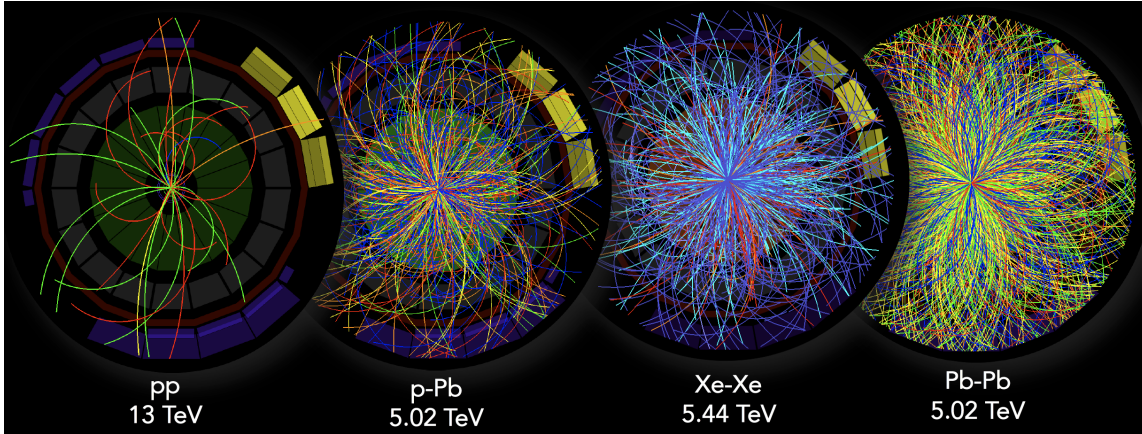


**Figure 1:** Typical event displays from the ALICE experiment at CERN showing various collision systems from pp (left) to Pb-Pb (right).

## 1. What is an ultra-relativistic nuclear collision?

The Large Hadron Collider (LHC) at CERN does not only collide protons on protons, but also heavier ions such as lead (Pb) or xenon (Xe). Approximately one month of running time per year is dedicated each year to these collisions. The energy released in such a collision can be quickly determined as follows. The top centre-of-mass energy in LHC Run 3 currently corresponds to  $\sqrt{s} = 13.6$  TeV. This corresponds to a beam energy of  $E_{beam} = 6.8$  TeV of a single proton. In a Pb-ion beam, however, only the protons in the Pb-nucleus get accelerated and not the neutrons. For a  ${}^{A=208}_{Z=82}\text{Pb}$ -isotope with  $Z = 82$  protons and in total  $A = 208$  nucleons, this results in a beam energy of  $E_{beam, PbPb} = 82/208 \cdot 6.8$  TeV = 2.68 TeV and correspondingly to a centre-of-mass energy per nucleon-nucleon pair of  $\sqrt{s_{NN}} = 5.36$  TeV.

Figure 1 shows typical event displays of these collisions in which the increase of particle multiplicity going from lighter to heavier colliding nuclei becomes immediately visible. The actual measurement of the total number of charged particles is routinely performed at the LHC and corresponds to about 22000 in central (small impact parameter) Pb-Pb collisions [1]. In our current understanding, the many re-scatterings among the partons created in the collision establish a local thermodynamic equilibrium soon after the initial nucleon-nucleon collisions. Naturally, this number of partons  $N$  is much smaller than the typical scale of thermodynamically described systems which is given by the Avogadro number, i.e.  $1 \ll N \ll 1$  mol. Nevertheless, it is still large enough to give access to new multi-body phenomena in QCD. Such a reasoning is best understood in analogy to QED: even knowing the Lagrangian of QED with precision, the wide areas of condensed matter or cold atom physics provide rich fields of study that are not immediately deducible from the fundamental interaction.

The main phenomenon to occur is the creation of the so-called quark-gluon-plasma (QGP) – a deconfined state of matter at very high temperatures [2, 3]. The QGP must exist at infinitely high temperatures as they were for instance present in the early universe. If we imagine a system of quarks and gluons at temperatures of e.g.  $T \gg 100$  GeV, then asymptotic freedom implies that any momentum transfer large enough to change the direction of such a particle is largely suppressed due

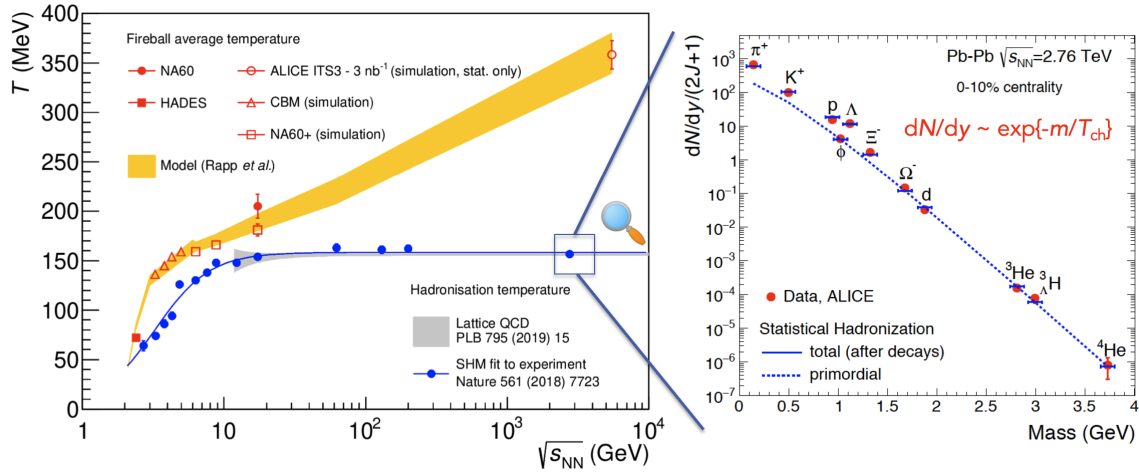


**Figure 2:** (Left panel) Average fireball temperature and hadronisation temperature as a function of collision energy in heavy-ion collisions. Figure taken from [7]. (Right panel) Thermal-statistical fit to particle yields. Figure taken from [8].

to the running coupling. Quarks and gluons must thus behave like a gas of free particles that are not localisable to individual hadrons anymore. At the same time, we know that at small temperatures, for instance the room temperature of around  $1/40$  keV, partons are confined into hadrons. Consequently, a phase transition between these regimes must occur at some intermediate temperature. Nowadays, lattice QCD calculations allow to pinpoint this phase transition to a critical temperature of around  $T \approx 150 - 160$  MeV, corresponding to about  $1.8 \cdot 10^{12}$  K [4]. In these calculations, the phase transition manifests itself as a fast rise in several observables such as the energy density or pressure. This fast rise is interpreted as a sudden increase in the number of degrees of freedom arising from the deconfined quarks.

Luckily, such temperatures are reached in ultra-relativistic heavy-ion collisions. They are for instance measured by determining the slope of the spectra of direct photons emitted from the fireball. In such studies, temperatures of around  $341 \pm 41$  MeV are obtained [5]. It must be noted though, that these measurements of direct photons remain of limited significance as the fast radial expansion leads to a blue-shift of the photon spectrum. Therefore, future experimental efforts are needed to allow for a model-independent determination of this temperature. This is possible by measuring the slope of the invariant mass spectrum of virtual photons that couple to di-leptons and are thus experimentally accessible. At the LHC, this will be feasible only in future thanks to the ITS2 and ITS3 upgrades [6].

While photons and di-leptons are sensitive to the average fireball temperature over its entire lifetime, the temperature after its hadronisation can be determined from systematic measurements of light flavour hadrons. This is demonstrated in the right panel of Fig. 2. In the statistical-thermal hadronisation model, the yields  $dN/dy$  are expected to be fully determined by their thermal equilibrium abundance, i.e. roughly proportional to the Boltzmann factor  $\exp(-m/T_{ch})$ , where  $m$  corresponds to the hadron mass and  $T_{ch}$  to the so-called chemical freeze-out temperature. The chemical freeze-out of the fireball is determined by the moment when the mean-free path for inelastic interactions exceeds its size. The experimentally determined value of  $T \approx 156$  MeV

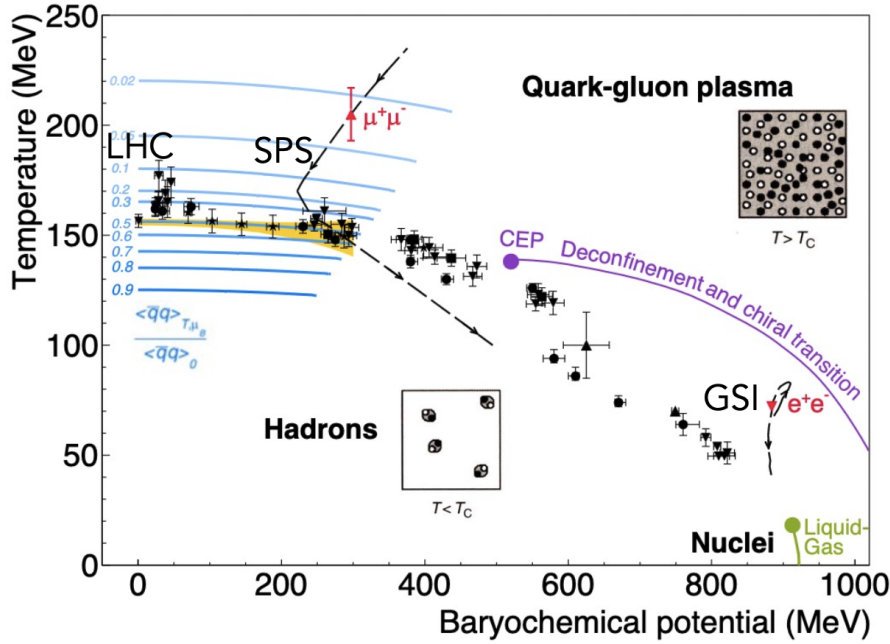


**Figure 3:** The phase diagram of strongly interacting matter. Figure taken from [11].

is consistent with the aforementioned lattice QCD calculations, thus indicating that the chemical freeze-out occurs soon after hadronisation.

The evolution of the temperatures occurring in heavy-ion collisions as a function of  $\sqrt{s_{NN}}$  is summarised in the left panel of Fig. 2. Notably, the hadronisation/chemical freeze-out temperature saturates above top SPS energies, i.e. any further increase in energy does not lead anymore to a higher *hadronic* temperature, but only to an increase of temperature in the partonic phase as evidenced by an increase in the average fireball temperature. While the latter is currently only predicted by model calculations [9], future experimental efforts will underlay these predictions for the so called *caloric curve of QCD* with precision data [6, 10].

## 2. Where do we do ultra-relativistic nuclear collision?

As already evident from the discussion on the caloric curve, heavy-ion physics naturally spans a wide range of collision energies. Broadly speaking, there is a high and a low energy frontier. The high energy frontier is currently at the LHC with all four major LHC experiments (ALICE, ATLAS, CMS, LHCb) pursuing very successful heavy-ion programs. The first heavy-ion run at the LHC took place in 2010 under the participation of ALICE, ATLAS, and CMS. It must be noted that the ALICE experiment is among the LHC experiments the one that is optimised for heavy-ion collisions. LHCb is taken heavy-ion data since the 2015 run.

At the low energy frontier, programs at several accelerators are either running or are planned in the current and next decade. Since many years, the Relativistic Heavy Ion Collider (RHIC) in Brookhaven contributes to the progress of the field. In particular, an ongoing beam energy scan aims at finding a critical point in the QCD phase diagram (see for instance [12] and references therein).

The FAIR facility in Darmstadt is planned to become operational in 2029. Several detectors that are currently operational (sPHENIX and STAR at RHIC, HADES at GSI, NA-61 at CERN-SPS) or planned (NA-60+ at CERN-SPS, CBM at FAIR, MPD at the NICA facility in Dubna) cover different regions in centre-of-mass energy and with different interaction rate [13]. The purpose of this effort is to shed light on the structure of the QCD phase diagram as shown in Fig. 3. Like water or any other chemical substance, also QCD has a phase diagram. Its control parameters are given by the temperature  $T$  and the baryochemical potential  $\mu_B$ . The latter quantifies the excess of baryons over antibaryons in the system.

### 3. What can we learn from ultra-relativistic nuclear collisions?

While the characterisation of the properties of the quark-gluon plasma in terms of its transport parameters such as the shear viscosity is the main goal of heavy-ion physics, recent developments also allowed intriguing insights into the neighboring fields of physics. These include the (subnucleonic) structure of nuclei as well as astroparticle physics. All in all, heavy-ion collisions provide a unique laboratory for many of these fields of study.

#### 3.1 Characteristics of the quark-gluon-plasma

The shear viscosity over entropy ratio  $\eta/s$  of the QGP is determined via the measurement of the anisotropic flow coefficients  $v_n$ . The  $v_n$ s are defined by the fourier decomposition of the particle multiplicities with respect to the  $n$ -th order reaction plane angle  $\Psi$  in the azimuthal plane:

$$\frac{dN}{d\phi} \propto 1 + 2 \sum_{n=1}^{\infty} v_n \cos[n(\phi - \Psi_n)] . \quad (1)$$

The spatial anisotropy of the initial state in non-central heavy-ion collisions induces a momentum anisotropy in the final state which is quantified by the  $v_n$ s. Fluctuations in the initial state lead to non-zero values of higher harmonics in the final state if they are not damped by the viscosity of the system. This results in a strong sensitivity of the  $v_n$  measurement to the viscosity. Nowadays, the most precise determinations of  $\eta/s$  use a plethora of data on  $v_n$  and particle production spectra and combine them in a Bayesian analysis (see for instance [14]). Remarkably, these studies find that the obtained values of  $\eta/s \approx 0.1 - 0.3$  are significantly smaller than that of any other known liquid, even superfluid helium. The QGP is therefore often referred to as an "ideal liquid".

Beyond its viscosity, another important transport parameter of the QGP is given by its diffusion coefficient. The diffusion of quarks inside the QGP is best studied using charm quarks. Charm quarks are roughly 200-500 times heavier than the much more abundant u- and d-quarks. That makes them so heavy that they are not produced thermally during the QGP lifetime ( $m_c \gg T$ ), but only in the initial nucleon-nucleon collisions where their abundance is calculable in perturbative QCD. Subsequently, their number is conserved during the further evolution of the system. The measurement of the  $v_2$  of D-mesons reveals a non-zero value indicating that they participate in the medium expansion: despite their heavy mass they receive so many kicks from the much more abundant u,d, and s-quarks that they thermalise [15, 16]. Based on model comparisons, one can then constrain the charm quark diffusion coefficient  $D_s$  to values of  $1.5 < 2\pi D_s T_c < 4.5$ . Charm quarks are therefore often considered to be the perfect tool to characterize the QGP medium in terms

of diffusion, recombination, and energy loss. Remarkably, a different behaviour is observed for the even heavier beauty quarks. Experimentally, one studies the difference in elliptic flow between prompt and non-prompt D-mesons, because the latter mostly originate from B-hadron decays. A significantly smaller  $v_2$  value is found for the non-prompt D-mesons [15, 16]. This indicates that b-quarks are only partially thermalised, i.e. that their relaxation time is significantly longer.

Given its importance for the field, a lot of the future physics program at the LHC is targeted at the reconstruction and study of heavy flavour hadrons. On one hand, the heavy-ion program in ATLAS, CMS, and LHCb will naturally profit from the planned Phase II upgrades of ATLAS and CMS as well as the LHCb upgrade II. On the other hand, a dedicated heavy-ion experiment ALICE 3 is planned for installation in Long Shutdown 4 [10]. The latter foresees a compact low mass all-silicon tracker with excellent vertex reconstruction and particle identification performance. The first layer is envisaged to be positioned inside the beam-pipe in only 5 mm distance from interaction point. In particular, this device will also allow for the reconstruction of multi-charm hadrons such as  $\Xi_{cc}$  in heavy-ion collisions.

The study of multi-charm particles follows the impressive developments that have been achieved over the last two decades in the quarkonium sector. As a matter of fact, the sequential suppression and regeneration of charm quarks is probably the most striking signature of deconfinement in the field. At SPS and RHIC energies, where the number of produced  $c\bar{c}$  pairs is small, de-confinement and subsequent scatterings yield to a separation of the  $c$  and  $\bar{c}$  quark that then hadronise into separate hadrons, most likely a  $D^0$  and  $\bar{D}^0$ . At LHC energies, the number of  $c\bar{c}$  pairs is so large that those originating from independent scatterings are re-combining leading to an enhancement over the original suppression [17]. This picture is further confirmed by the behaviour of Bottomonia that are more rarely produced and remain suppressed also at LHC energies [18]. Remarkably, less tightly bound states such as  $\Upsilon(3s)$  are more suppressed than the more tightly bound states such as  $\Upsilon(1s)$  [19].

Another striking indication for QGP formation in heavy-ion collisions is the phenomenon of jet quenching. Fig. 4 shows an example event with a roughly 300 GeV jet on one side of the collision and the away-side jet being absorbed in the roughly 10 fm of QCD medium. Many quantitative studies related to such observations aim at understanding the details of energy loss mechanisms of partons in the medium and the determination of the so-called  $\hat{q}$  variable that quantifies the energy loss per unit path length. One example of such studies is given by the distribution of  $x_j = p_T^{\text{subleading}} / p_T^{\text{leading}}$  which monitors the transverse momentum of the subleading jet with respect to the one of the leading jet in the event. While in pp collisions, the distribution is naturally peaked close to unity, it is peaked around 0.6 in Pb–Pb collisions [20, 21]. The ideal probe for such studies are clearly jet-photon measurements in which the leading jet is given by a highly energetic photon that escapes the medium without re-interaction. While current studies are still somewhat statistically limited [22], future LHC heavy-ion runs will elucidate the picture [23].

### 3.2 (Subnucleonic) Structure of nuclei

The LHC collides lead ions that are fully stripped, i.e. ions of the type  $^{208}\text{Pb}^{82+}$  that are 82 times positively charged. The strong electromagnetic field surrounding the nucleus results in photon-Pb collisions which probe the (subnucleonic) structure of the nucleus. In particular, the coherent  $J/\psi$  production probes the low Bjorken- $x$  gluon parton distribution functions *inside* the

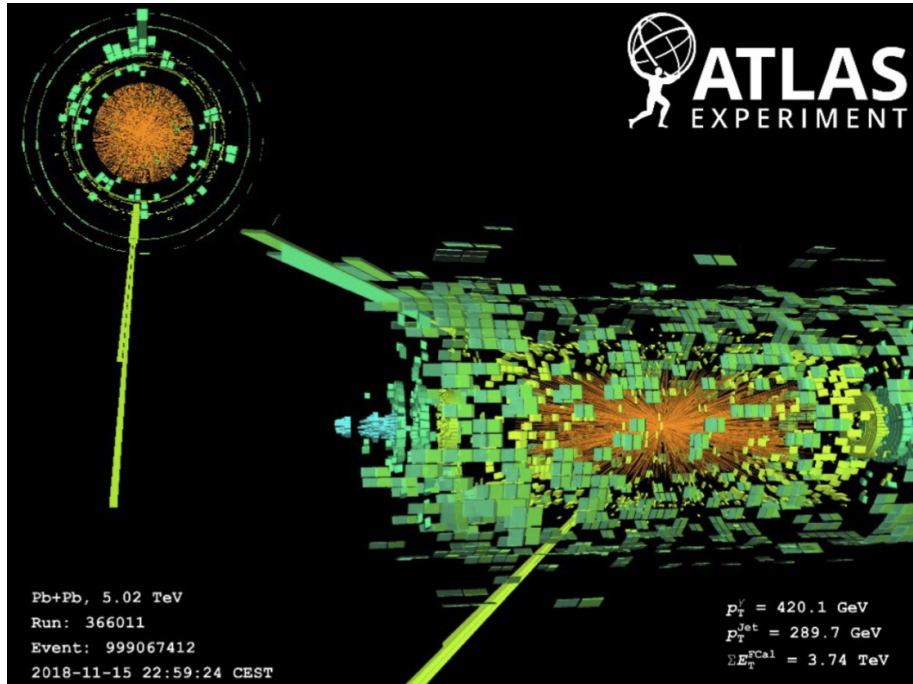


**Figure 4:** Event display from the ATLAS experiment showing a quenched jet.

nucleus. A comparison of the observed cross-section with the impulse approximation (no nuclear effects) allows for the extraction of the so called gluon shadowing factor, i.e.  $R_g \approx 0.5$  at  $x \approx 10^{-5}$ .

Another interesting study is focused on the determination of the neutron skin of nuclei based on ultra-relativistic heavy-ion collisions [24]. The collision deposits energy in the interaction region depending on the extent of the neutron skin in the  $^{208}\text{Pb}$  nuclei. A larger neutron skin leads to a considerably larger total hadronic cross section  $\sigma_{tot}$  and the resulting QGP droplet is in addition more diffuse and less elliptical. By a careful study of all relevant observables, one is thus able to constrain the size of the neutron skin with a precision that is comparable to more traditional methods and state-of-the-art calculations.

### 3.3 Astroparticle physics

One of the most exciting topics in modern physics is the search for dark matter. One of the main hypotheses for its nature is the weakly massive interacting particle (WIMP). Some of these proposed dark matter candidates are expected to annihilate into  $^3\text{He}$  particles. These particles are actively searched for in space- and balloon-borne experiments such as AMS or GAPS. At the same time, collider based experiments are needed for a to understand (i) antinuclei formation mechanisms in order to model production in dark matter decays, (ii) antinuclei formation mechanisms in order to model production in background reactions from collisions of ordinary cosmic rays, and (iii) the interaction of antinuclei with ordinary matter to determine the transparency of the galaxy. At the LHC, both the ALICE and LHCb experiment contribute to these activities. Thanks to its excellent particle identification capabilities, ALICE is well suited to measure production and annihilation cross-sections of  $\bar{p}$ ,  $\bar{d}$ , and  $^3\bar{\text{He}}$ . The LHCb experiment also uses the so-called SMOG system for fixed target collisions that can very well model cosmic ray collisions by studying p-He collisions.

It is in addition very well suited to study  $\bar{p}$  production thanks to its good particle identification capabilities. In particular, it is also able to measure prompt and non-prompt contributions in antiproton production [25]. Such studies are of great importance to reduce uncertainties in modeling the antiproton flux near earth that shows a roughly  $1\sigma$  excess above known sources [26]. Remarkably, new studies show that also  ${}^3\bar{\text{He}}$  can be identified based on the energy loss in the VELO detector.

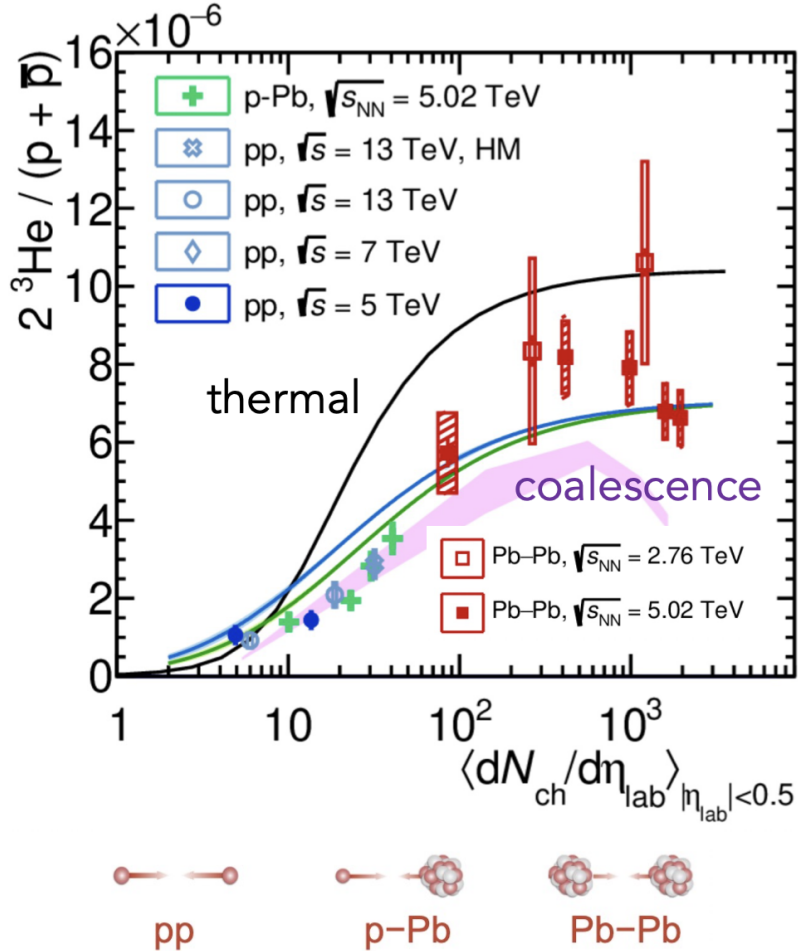


**Figure 5:** Production yield of  ${}^3\bar{\text{He}}$  as a function of event multiplicity as measured by ALICE in comparison to production model. Figure taken from [27].

In this context, proton-proton and heavy-ion collisions at the LHC serve as a "anti-matter factory" that allows many unique studies. As shown in Fig. 5, the measurements from small (pp) to large (Pb-Pb) collision systems allows to constrain the production mechanisms of light antinuclei such as  ${}^3\bar{\text{He}}$  [27]. The two main mechanisms under consideration, statistical-thermal and coalescence, give a different prediction for the production yield as a function of event multiplicity and thus can be distinguished. The antinuclei produced in the collision then travel through the detector where they might interact hadronically with the material. This fact allows to infer these unknown cross-sections that are also needed to determine the mean free path of antinuclei in the universe [28]. These studies indicate that only about 50% of the  ${}^3\bar{\text{He}}$  nuclei that are potentially

produced by dark matter annihilations in the centre of the galaxy would annihilate with the intergalactic matter on their travel to earth.

#### 4. Summary

Ultra-relativistic collisions are a unique laboratory to study QCD at extreme densities. A World-wide program involving many facilities and collaborations is needed to study the phase diagram of QCD in all its facets. The characterization of the QGP enters a quantitative era (numerical determination of transport coefficients) and will reach textbook quality in the next decade. Along the way, many interesting and unique insights impacting the neighboring fields of nuclear and astroparticle physics have been found.

#### References

- [1] ALICE collaboration, *Centrality dependence of the pseudorapidity density distribution for charged particles in Pb-Pb collisions at  $\sqrt{s_{NN}} = 5.02$  TeV*, *Phys. Lett. B* **772** (2017) 567 [1612.08966].
- [2] J.C. Collins and M.J. Perry, *Superdense Matter: Neutrons Or Asymptotically Free Quarks?*, *Phys. Rev. Lett.* **34** (1975) 1353.
- [3] N. Cabibbo and G. Parisi, *Exponential Hadronic Spectrum and Quark Liberation*, *Phys. Lett. B* **59** (1975) 67.
- [4] HotQCD collaboration, *Equation of state in (2+1)-flavor QCD*, *Phys. Rev. D* **90** (2014) 094503 [1407.6387].
- [5] ALICE collaboration, *Direct photon production in Pb-Pb collisions at  $\sqrt{s_{NN}} = 2.76$  TeV*, *Phys. Lett. B* **754** (2016) 235 [1509.07324].
- [6] L. Musa, *Letter of Intent for an ALICE ITS Upgrade in LS3*, Tech. Rep. , CERN, Geneva (2019), DOI.
- [7] T. Galatyuk and A. Kalweit, *Github repository for caloric curve summary plot* [https://github.com/tgalatyuk/qcd\\_caloric\\_curve](https://github.com/tgalatyuk/qcd_caloric_curve), 2021.
- [8] A. Andronic, P. Braun-Munzinger, K. Redlich and J. Stachel, *Decoding the phase structure of QCD via particle production at high energy*, *Nature* **561** (2018) 321 [1710.09425].
- [9] R. Rapp, H. van Hees and M. He, *Properties of Thermal Photons at RHIC and LHC*, *Nucl. Phys. A* **931** (2014) 696 [1408.0612].
- [10] ALICE collaboration, *Letter of intent for ALICE 3: A next-generation heavy-ion experiment at the LHC*, 2211.02491.
- [11] HADES collaboration, *Probing dense baryon-rich matter with virtual photons*, *Nature Phys.* **15** (2019) 1040.

- [12] X. Luo and N. Xu, *Search for the QCD Critical Point with Fluctuations of Conserved Quantities in Relativistic Heavy-Ion Collisions at RHIC : An Overview*, *Nucl. Sci. Tech.* **28** (2017) 112 [1701.02105].
- [13] T. Galatyuk, *Future facilities for high  $\mu_B$  physics*, *Nucl. Phys. A* **982** (2019) 163.
- [14] J.E. Bernhard, J.S. Moreland and S.A. Bass, *Bayesian estimation of the specific shear and bulk viscosity of quark–gluon plasma*, *Nature Phys.* **15** (2019) 1113.
- [15] ALICE collaboration, *Measurement of Non-prompt  $D^0$ -meson Elliptic Flow in Pb-Pb Collisions at  $\sqrt{s_{NN}} = 5.02$  TeV*, 2307.14084.
- [16] CMS collaboration, *Measurements of azimuthal anisotropy of nonprompt  $D^0$  mesons in PbPb collisions at  $\sqrt{s_{NN}} = 5.02$  TeV*, 2212.01636.
- [17] ALICE collaboration,  *$\psi(2S)$  suppression in Pb-Pb collisions at the LHC*, 2210.08893.
- [18] ALICE collaboration,  *$\Upsilon$  production and nuclear modification at forward rapidity in Pb–Pb collisions at  $s_{NN}=5.02$ TeV*, *Phys. Lett. B* **822** (2021) 136579 [2011.05758].
- [19] CMS collaboration, *Observation of the  $\Upsilon(3S)$  meson and suppression of  $\Upsilon$  states in PbPb collisions at  $\sqrt{s_{NN}} = 5.02$  TeV*, 2303.17026.
- [20] ATLAS collaboration, *Measurements of the suppression and correlations of dijets in Pb+Pb collisions at  $s_{NN}=5.02$  TeV*, *Phys. Rev. C* **107** (2023) 054908 [2205.00682].
- [21] ATLAS collaboration, *Measurements of the suppression and correlations of dijets in Xe+Xe collisions at  $s_{NN}=5.44$  TeV*, *Phys. Rev. C* **108** (2023) 024906 [2302.03967].
- [22] CMS collaboration, *Groomed jet radius and girth of jets recoiling against isolated photons in PbPb and pp collisions at 5.02 TeV*, .
- [23] Z. Citron et al., *Report from Working Group 5: Future physics opportunities for high-density QCD at the LHC with heavy-ion and proton beams*, *CERN Yellow Rep. Monogr.* **7** (2019) 1159 [1812.06772].
- [24] G. Giacalone, G. Nijs and W. van der Schee, *Determination of the Neutron Skin of Pb208 from Ultrarelativistic Nuclear Collisions*, *Phys. Rev. Lett.* **131** (2023) 202302 [2305.00015].
- [25] LHCb collaboration, *Measurement of antiproton production from antihyperon decays in pHe collisions at  $\sqrt{s_{NN}} = 110$  GeV*, *Eur. Phys. J. C* **83** (2023) 543 [2205.09009].
- [26] G. Giesen, M. Boudaud, Y. Génolini, V. Poulin, M. Cirelli, P. Salati et al., *AMS-02 antiprotons, at last! Secondary astrophysical component and immediate implications for Dark Matter*, *JCAP* **09** (2015) 023 [1504.04276].
- [27] ALICE collaboration, *Light (anti)nuclei production in Pb-Pb collisions at  $s_{NN}=5.02$  TeV*, *Phys. Rev. C* **107** (2023) 064904 [2211.14015].
- [28] ALICE collaboration, *Measurement of anti- $^3\text{He}$  nuclei absorption in matter and impact on their propagation in the Galaxy*, *Nature Phys.* **19** (2023) 61 [2202.01549].